Journal of Physics: Conference Series

PAPER • OPEN ACCESS

The discovery of gravitational waves: a gentle fight against noise

To cite this article: Giancarlo Cella 2017 *J. Phys.: Conf. Ser.* **880** 012007

IOP Conf. Series: Journal of Physics: Conf. Series **880** (2017) 012007 doi:10.1088/1742-6596/880/1/012007

The discovery of gravitational waves: a gentle fight against noise

Giancarlo Cella

INFN Sez. Pisa – Largo B. Pontecorvo 3 56127 Pisa (Italy)

E-mail: giancarlo.cella@pi.infn.it

Abstract. The recent direct observation of gravitational waves coming from collisions between black holes is the fulfillment of a dream started more than sixty years ago with the pioneering experiments of J. Weber. This has been possible by reaching with interferometric detectors an unprecedented sensitivity, which requires the reduction of several technical and fundamental noise sources, thermal and quantum in particular. I discuss some of these, with some emphasis on quantum noise. I also briefly discuss the first detection results and their impact on fundamental physics, commenting about future perspectives and challenges.

1. Introduction

Albert Einstein elaborated general relativity motivated by the exigence of having a theory of gravitation not in conflict with special relativity. This was not the case of Newtonian theory, where gravity is an action at distance analogous to the Coulomb force in electromagnetism. Following this analogy, general relativity could be understood as a theory for a field which should play a similar role of electric and magnetic field in Maxwell's theory.

As shown by Einstein himself [1], the theory allows for wave-like solutions which are generated by accelerated mass motion (or, more generally, by energy momentum tensor as should be for a relativistic theory). Compared with electromagnetic interaction, the gravitational one has some peculiarities. By choosing appropriately the reference frame the gravitational effects can always be set to zero at a given event in space-time. This is the so-called equivalence principle which Einstein took as a cornerstone of his theory, and allows for a geometric interpretation: gravitational effects are due to space-time curvature, and the space-time metric tensor $g_{\mu\nu}$ play the role of the gravitational field.

As the source of gravitation is the energy-momentum tensor, it is expected that gravitational field should contain energy itself and must behave as a source for itself, in other words general relativity should be a nonlinear theory. All this is nicely described by the Einstein equation

$$G_{\mu\nu} = \frac{8\pi G}{c^4} T_{\mu\nu} \tag{1}$$

where $G_{\mu\nu}$ is a tensor which depends in a nonlinear way from the metric and its first and second derivatives, G the Newton's constant and c the speed of light.

The nonlinear character of the theory, and its covariance with respect to arbitrary changes of coordinates, triggered subtle controversies about the interpretation of their wave-like solutions, which can be obtained naively by adding a small perturbation $h_{\mu\nu}$ to the flat space solution described by the Minkowski metric $\eta_{\mu\nu}$

$$g_{\mu\nu} = \eta_{\mu\nu} + h_{\mu\nu} \tag{2}$$

and by linearizing Equation (1). In an appropriate coordinate system this gives an equation for waves which propagates at speed of light, with two independent polarizations.

At some point, Einstein himself was not convinced about the real existence of gravitational waves. He submitted together with Nathan Rosen a paper to Physical Review titled "Do the gravitational waves exist?". The paper was rejected, to great Einstein's disappointment, and then resubmitted [2] and published in another journal. After several decades of discussions a general consensus about the existence of gravitational waves was reached, and in particular about the back action effects of gravitational wave emission on the source. Appropriate approximation schemes for calculations were developed, starting from Einstein-Infeld-Hoffmann equations [3], which are appropriate for a source in slow motion.

An indirect experimental confirmation for the existence of gravitational waves came from the observation of the binary pulsar PSR B1913+16 by Hulse and Taylor [4]. The observed decrease of the orbital period of the system in very good agreement with the expectation of general relativity for the rate of energy loss.

The dominant contribution to a gravitational wave generated by this kind of source can be estimated as

$$h_{ij} \simeq \frac{1}{r}\frac{2G}{c^4}\ddot{Q}_{ij}^{TT} \tag{3}$$

where Q_{ij} is the transverse and traceless part of the quadrupole momentum of the source and h_{ij} the adimensional strain generated by it. The strain h_{ij} is a measurement of the effect of the wave, and can be understood as a relative change of length. Looking at the smallness of the prefactor, it can be realized that a $\ddot{Q}_{ij}^{TT}$ large enough to be directly detectable can be provided only by astrophysical (or cosmological) sources. Still, estimates of the expected h_{ij} give typically values $O\left(10^{-22}\right)$ or less.

A large enough sensitivity is currently reached by interferometric detectors such as Advanced LIGO [5] and Advanced VIRGO [6]. The basic detection principle is the accurate measurement of the difference between the lengths of the two arms of a Michelson interferometer (see Figure 1). A laser beam is injected in the system, and separated in two parts using a partially reflecting mirror (the beam splitter BS). The two beams obtained are then recombined after they traveled in the two arms, and a relative change of the arm lengths generate a relative phase shift which is detected at the output B1.

In order to increase the sensitivity a Fabry-Perot resonant cavity is built inside each arm. The length scale L of each arm is 4km for Advanced LIGO (3km for Advanced VIRGO): this means that the length sensitivity of the apparatus must be of the order of $Lh \simeq 4 \times 10^{-19}$, which is a fraction of the diameter of a proton. This is possible only by maintaining all the noise sources which couples to the detector at a low enough level.

2. Sources

There are several potential sources of detectable gravitational waves. A possible classification is based on the peculiarities of the expected signal: roughly speaking we can speak about *chirps, bursts, continuous signals and stochastic signals.*

A *chirp-like* signal is expected in compact binary coalescence events. They can be described as the last part of the evolution for a bound system of two compact objects of masses m_1 and m_2 (black holes or neutron stars). As in the case of the PSR B1913+16 binary system, the two orbiting bodies generates a $\ddot{Q}_{ij} \neq 0$, and radiates gravitational waves loosing energy. During this process the relative distance between the bodies decreases, and the orbital frequency increases. If

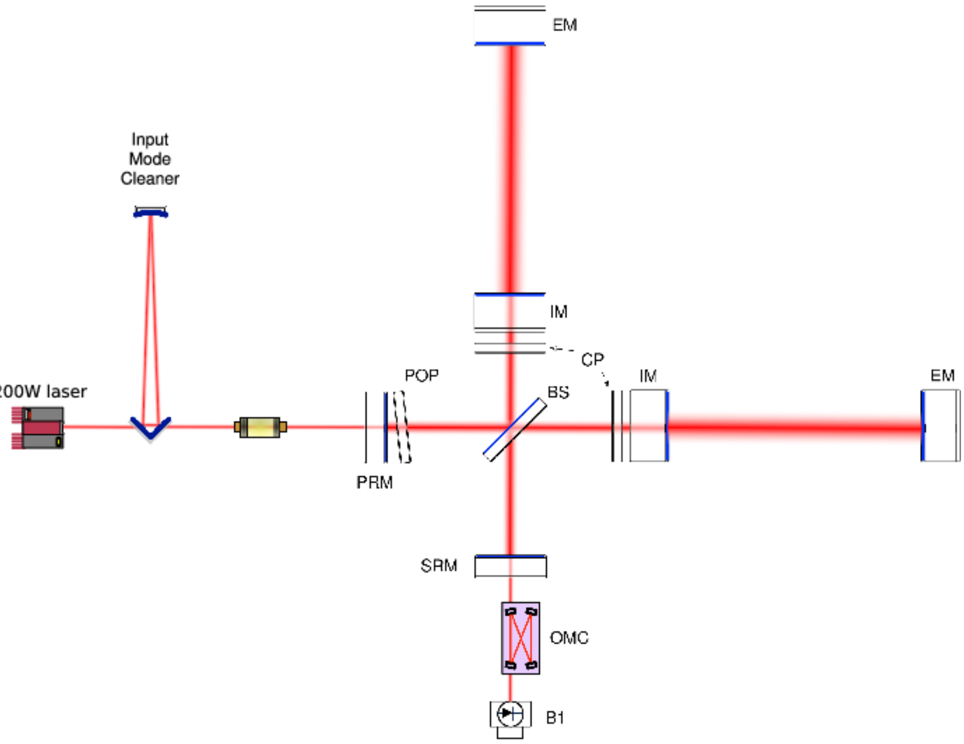

Figure 1. A simplified optical scheme of Advanced VIRGO [6]. The basic topology is the one of a Michelson interferometer. In each arm a resonant Fabry-Perot optical cavity is built (IM-EM mirrors). Power recycling (PRM) and signal recycling (SRM) mirrors are added to increase sensitivity.

we exclude the final part of the evolution we can neglect relativistic and strong field corrections: the relative energy loss for each orbit is small and we can describe the process in the adiabatic approximation. The result is a quasi-periodic signal, which can be written as

$$h_{ij} \sim \frac{4}{r}\left(\frac{GM_c}{c^2}\right)^{5/3}\left(\frac{\omega_{gw}(t)}{2c}\right)^{2/3}\cos\left[\Phi_0 + \int^t \omega_{gw}(t')dt'\right] \tag{4}$$

neglecting an angular factor which depends on the polarization and on the source position in the sky. Here $M_c = (m_1 m_2)^{3/5}(m_1+m_2)^{-1/5}$ is the chirp mass of the system and $\omega_{gw}(t)$ is the instantaneous angular frequency of the wave, which is two times the orbital angular frequency, owing to its quadrupolar nature. We see that both the frequency and the amplitude of the signal increases accordingly with the law

$$\omega_{gw}(t) = \frac{1}{4}\left(\frac{GM_c}{c^3}\right)^{-5/8}\left(\frac{5}{t_c - t}\right)^{3/8} \tag{5}$$

When $t = t_c$ both the amplitude and the frequency diverges. Before that the relative distance between the two bodies become so small that they merge together. This process cannot be described using a simple analytical approximation but requires numerical simulations which fully take into account strong field effects in general relativity: anyway t_c is called coalescence time and can be used as an estimate for the time of merger. Equation (5) will be an acceptable approximation only until[1]

$$f_{gw} \lessapprox f_{\rm ISCO} = 2.2 \times 10^3 {\rm Hz} \left(\frac{M_\odot}{m_1 + m_2} \right) \tag{6}$$

which we can take as an upper limit for the frequencies emitted by the source.

In the case of the Hulse-Taylor pulsar $\omega_{gw} \simeq 2 \times 10^{-4}$s: this means that the frequency of the gravitational wave emitted is too small to be detectable by VIRGO and LIGO, which as we will see have a good sensitivity in the frequency band between $O(10)$ Hz and $O(10^4)$ Hz. It means also that PSR B1913+16 will merge in $O(10^8)$ years: in the final phase for the system evolution the signal will enter in the detection bandwidth of the detectors, and will stay there until $f_{\rm ISCO}$ will be reached.

Note the inverse proportionality between $f_{\rm ISCO}$ and the mass of the system. This means that if the total mass of the system is large the merger will happen when the signal is inside the detection band. When the total mass increases, the time spent inside the detector's sensitivity window will decrease until it will disappear completely.

A *burst* signal is characterized by its small duration, typically of the $O(10^{-2})$s. They can be produced in violent explosive events, such as a *supernovae* explosions but also in some more exotic cases, for example in cosmic string dynamics.

In the case of *supernovae*, a requirement for the generation of gravitational wave is that the core collapse must be asymmetric, otherwise no quadrupole or higher time dependent moment can be generated. There is no clear consensus about the asymmetry one can expect, as the physics involved is quite intricate and large scale numerical simulations are needed. An *supernova* event in our galaxy is expected once in $10 - 100$y, so the chances of observing it are not very high. However if this will happen the study of the emitted signal could add a lot to the knowledge of this still poorly understood physical system.

Continuous signals can be produced by a rotating neutron star. This very compact object (a mass typically of about $1.4M_\odot$ is confined in a region with a radius of few kilometers) can generate gravitational waves if a small deviation from sphericity is present. This can be allowed by elastic or magnetic effects in the crust, and the expected deviation are quite small. However a signal of this kind could help, if detected, in clarifying the nature of the matter inside the star, and in particular its equation of state [7].

Finally a *stochastic signal* can be generated by a superposition of several events, both of astrophysical or cosmological origin. It is called stochastic because, owing to the large overlap between different contributions, it is not possible to resolve the single event. As a consequence it is not possible to describe it using a deterministic theoretical waveform to be searched for, maybe parametrized by a set of unknown parameters as is the case for a *chirp* or for a continuous signal. Instead the signal must be modeled as a stochastic process, and is characterized by their statistical properties such as the time correlation functions.

One consequence of this is that in order to detect a stochastic background of gravitational waves more than one detector is needed. The basic strategy is to estimate the correlation between the output of a pair of detectors. Under the hypothesis that the two noises are uncorrelated (which should not be taken as granted, especially if the detectors are one near the other) this allows for a detection or, at least, to the definition of an upper limit.

An astrophysical stochastic background could be the cumulative superposition of many binary coalescence events, or many bursts, or many continuous signals. Its detection could give interesting information about the validity of stellar evolution models.

A cosmological stochastic background can be the result of processes happened in the first phase of the universe, such as inflation, phase transitions, cosmic string network evolution. They

[1] This estimate of $f_{\rm ISCO}$ is strictly valid only when one mass is much smaller than the other, and neglects spin effects.

are in principle very interesting because, owing to the weakness of gravitational interaction, the universe can be considered transparent for gravitational wave radiation since its beginning, so the gravitational waves generated can propagate unperturbed toward the present epoch. For this reason the detection of a cosmological stochastic background of gravitational waves could give a unique opportunity for getting information about the very young universe [8].

Currently there are three gravitational wave detectors of comparable sensitivity, the two of the LIGO Advanced project in USA, and the VIRGO Advanced in italy, near Pisa. Only the first two where running during the first direct detection, while VIRGO is expected to join in august 2017. The availability of several detectors is important from several point of view. As we saw in the case of stochastic background at least a pair of detector is mandatory.

Ideally the experimental noise can be described as a Gaussian stochastic process. If this is the case the detection probability can be increased also for a deterministic signal by combining together in a coherent way the measurements of all the available detectors. In a realistic situation, where the statistical characterization of the experimental noise is never completely under control, the request for a coincident detection increases the confidence on the result.

A signal from a source at a given position in the sky and with a given polarization couples in a different way to detectors with different location and orientation. Using several detectors at the same time allows for the determination of the source position, mainly by looking at the relative delays observed between the signals to do a triangulation. In this case, at least three detectors are needed to solve the problem and to determine the coordinates in the sky, with an accuracy which depends also, of course, on the signal to noise ratio. This is quite important because in many cases a non gravitational counterpart of the event is expected. For example, a binary coalescence between two neutron stars is expected to be a trigger for a gamma ray burst, and it is important to localize accurately the source, in a time as short as possible, to allow for a complementary electromagnetic observation.

Another interesting application of a multidetector analysis is the determination of the polarization of the gravitational wave, which allows for a more accurate determination of the source parameters and is an important test for the validity of general relativity. This is because extended models for theory of gravitation allows, quite generically, additional polarizations beside the canonical two foreseen by Einstein's theory.

3. A fight against the noise

The simplest characterization of the sensitivity of a gravitational wave detector can be given by its strain equivalent amplitude noise spectrum. The idea is to normalize the detector's output $s(t)$ in such a way that

$$s(t) = h(t) + n(t) \tag{7}$$

where $h(t)$ is the gravitational strain and $n(t)$ the noise. If the noise is stationary the power spectrum of $n(t)$ can be written as

$$\left\langle \tilde{n}(\omega)^* \tilde{n}(\omega') \right\rangle = 2\pi\delta\left(\omega - \omega'\right) S_n(\omega) \tag{8}$$

and the strain equivalent noise spectrum is just given by $\sqrt{S_n}$. The noise budget planned for Advanced VIRGO is plotted in Figure 2. The best sensitivity window is between 20Hz and 4×10^3kHz. We see also that the dominant source of noises are the thermal one (below 300Hz) and the quantum one, in the higher frequency region.

Seismic noise does not appear in the picture, but becomes the main limit below 10Hz. Special care is taken to attenuate it, the reason being that the typical spectral amplitude of the motion of the surface of the earth is at least nine orders of magnitude larger than the expected signal in the detection bandwidth. The principle used for seismic noise attenuation in VIRGO is based on a chain of oscillators which are interposed between the ground and the suspended mirror. They

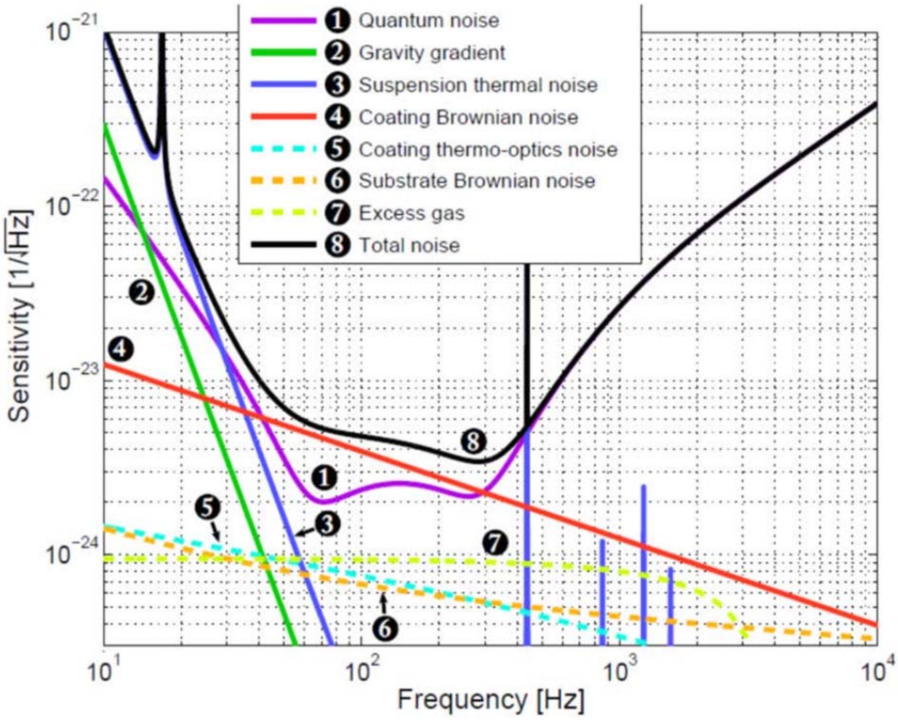

Figure 2. The strain equivalent spectral amplitudes $\sqrt{S_n(\omega)}$ of several noises coupled to VIRGO Advanced, as a function of the frequency. Most relevant contributions comes from quantum noise and from thermal noise of mirror coating and suspensions. Seismic noise dominates below 10Hz and is not represented.

are designed in such a way that the proper frequencies ω_p of the chain are below 1Hz. Above these the oscillator chain spectral transfer function is depressed by a factor $\left(\frac{\omega_p}{\omega}\right)^{2n}$, where n is the number of stages. With a large enough n the required attenuation factor can be reached. Currently $O(10^{-15})$ attenuation factors can be obtained in this way.

The main target for second generation (advanced) detectors was the improvement of the best sensitivity of one order of magnitude in h. This will be obtained (when the design sensitivity will be reached) mainly by reducing thermal and quantum noise. I will give come details about quantum noise in the next section, and I concentrate here on thermal noise.

Thermal noise is the unavoidable result of the coupling between the apparatus and the environment. When the system is in thermodynamical equilibrium its thermal fluctuations can be evaluated by using the fluctuation-dissipation theorem. This theorem told us that the spectral amplitude of thermal noise is proportional to dissipative effects.

In an interferometric detector we are interested in the phase fluctuations induced by the thermal agitation of the mirror surface on the laser beam. There are essentially three different possibilities for reducing them:

(i) The thermodynamical way. Thermal noise amplitude is proportional to the square root of the temperature, so it is possible to reduce it with a cryogenic setup. This is not easy, especially because the cryogenic infrastructure can reintroduce other kind of noises, such as mechanical vibration. Beside that, a non trivial problem is the elimination of the heat which is transferred by the laser to the mirrors. This is a small fraction of the total power, as a large effort is done to use mirrors with a very low absorption, but can become significant if

IOP Conf. Series: Journal of Physics: Conf. Series **880** (2017) 012007 doi:10.1088/1742-6596/880/1/012007

the laser power is very high. Neither VIRGO Advanced nor LIGO Advanced are cryogenic experiments.

(ii) The statistical way. The total phase shift of the laser beam is an average of the mirror displacement weighted by the laser intensity profile. A direct way to reduce thermal fluctuations is to use larger beams, which average more. There are however some limitations, because the dimension of a beam is limited by the mirror size and it is not possible to increase this by a large factor.

(iii) The material improvement way. By optimizing the material and the mechanical construction we can reduce the source of dissipation, which are a measurement of the coupling between the system and the environment. The largest contribution to thermal noise comes currently from the optical coating of the mirrors, which is needed to obtain the requested reflectivities (very large or very small, as needed). But the mechanical properties of the materials used for the coating are not good enough, and there is an intense activity in searching for better materials and solutions.

One of the main difficulty in the thermal noise reduction program is about the strong interdependence between possible solutions and other requirements, such as mechanical and optical properties of the apparatus.

4. Quantum noise

Looking at Figure 2 we see above 300Hz the sensitivity is limited by the so-called quantum noise. In this high frequency region this is commonly called "shot noise", and is connected with the quantum nature of light.

The most direct way to decrease the shot noise is to increase the laser power. However this solution is not a free lunch: a more powerful laser can introduce problems connected with thermal lensing and power absorption which can be quite difficult to solve, such as the parametric resonance one [9]. An alternative is based on the use of squeezed light, as I will discuss next.

In future detectors thermal noise will be reduced further. The impact of quantum noise will be more and more important at intermediate frequencies, and its subtle nature will come out.

4.1. An example: optical cavity

A crude model for a laser beam, which however is good enough to understand several peculiarities of ponderomotive effects in interferometers, is a plane wave with some given frequency ω_0. When this plane wave interacts with optical elements such as a moving mirror or a beam splitter it is reflected and modulated. We will write the classical electric field at a given point as the first component of the bidimensional vector

$$\boldsymbol{E}(t) = \mathbb{R}\left(\omega_0 t\right) \boldsymbol{e}(t) \tag{9}$$

Here $\mathbb{R}(\theta)$ is a rotation matrix by an angle θ and $e_i(t)$ are functions with a slow variation on the timescale ω_0^{-1}. When modulations effect are small, we can write Eq. (9) in a slightly different way

$$\boldsymbol{E}(t) = \mathbb{R}\left(\omega_0 t\right) \left[\overline{\boldsymbol{e}} + \delta \boldsymbol{e}(t)\right] \tag{10}$$

with $|\delta \boldsymbol{e}| \ll |\overline{\boldsymbol{e}}|$. In this way we emphasize the separation between the ideal, monochromatic plane wave contribution $\overline{\boldsymbol{e}}$ and the small corrections $\delta \boldsymbol{e}$ which carry the relevant information coming from the detector, both the signal and the noise.

This is the basic idea beyond the graphical representation in Figure 3. The average part $\mathbb{R}\overline{\boldsymbol{e}}$ is represented by the black sticks, rotating with angular frequency ω_0, the "fluctuating" one $\mathbb{R}\delta\boldsymbol{e}(t)$ by the gray "balls". From this graphical representation it is easy to understand that the component of the fluctuating vector $\delta \boldsymbol{e}$ parallel to $\overline{\boldsymbol{e}}$ represents the amplitude fluctuation

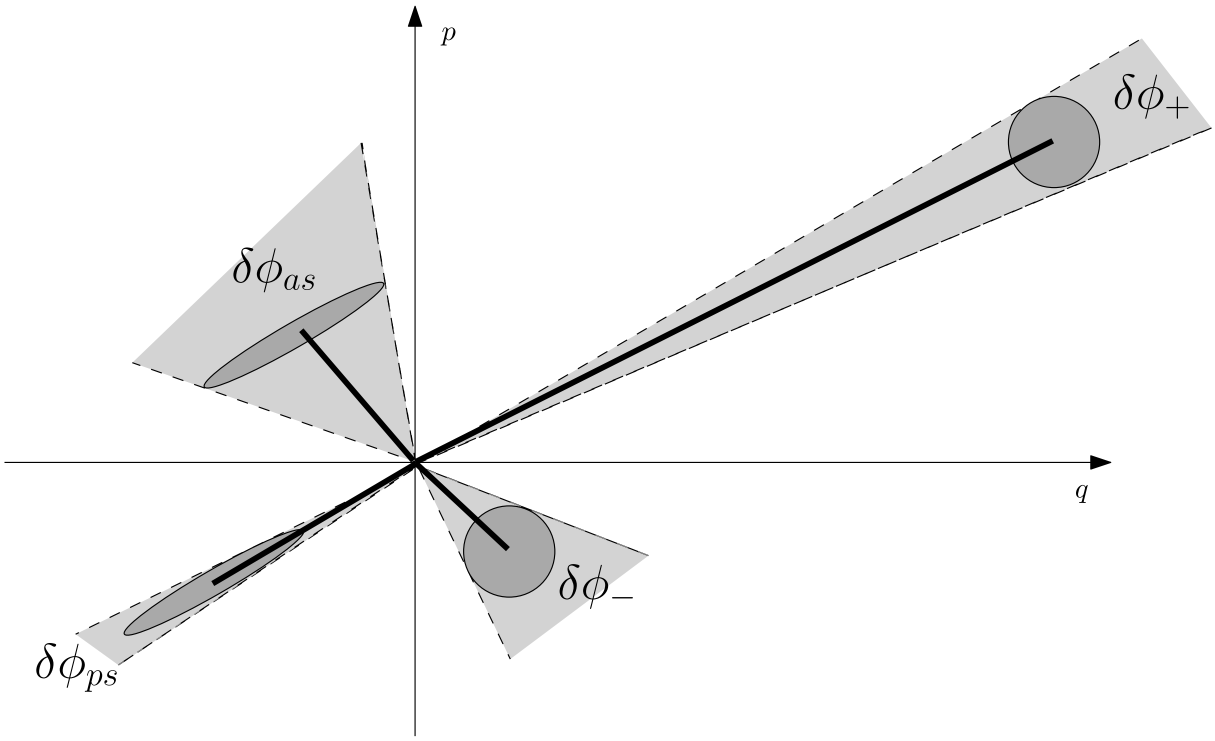

Figure 3. A graphic representation of the field described by Equation (10). The black stick represents the "average" part of the field (which is monochromatic with angular frequency ω_0). The dark gray areas represent the fluctuating parts of the field: they can be seen as the typical region where the field can be found. It follows that the light gray regions are estimates of phase fluctuation.

of the field, and the perpendicular component is proportional to the phase fluctuation, namely $\delta\phi(t) \sim |\overline{\boldsymbol{e}}|^{-2} |\delta\boldsymbol{e} \wedge \overline{\boldsymbol{e}}|$.

It is easy to understand how the modulation vectors which describe the field at different points are related. For example, after a free propagation over a length ℓ the field is simply delayed by ℓ/c, which means

$$\overline{\boldsymbol{e}}' + \delta\boldsymbol{e}'(t) = \mathbb{R}\left(\frac{\omega_0\ell}{c}\right)\left[\overline{\boldsymbol{e}} + \delta\boldsymbol{e}\left(t - \frac{\ell}{c}\right)\right] \tag{11}$$

Note that the fluctuating part is not simply rotated, but it gets an additional delay.

The most important rule from our point of view is the one that gives the field reflected on a moving mirror. In the context of interferometric detectors the mirror's displacement from his reference position $\delta z(t)$ is slow and small. By assuming it of the same order of field's fluctuation in the linear approximation we obtain from (11)

$$\overline{\boldsymbol{e}}' + \delta\boldsymbol{e}'(t) = \mathbb{R}\left(\omega_0\delta\tau\right)\left[\overline{\boldsymbol{e}} + \delta\boldsymbol{e}\left(t - \delta\tau\right)\right] \simeq \overline{\boldsymbol{e}} + \delta\boldsymbol{e}\left(t\right) + \frac{\omega_0\delta\tau}{c}\mathbb{R}\left(\frac{\pi}{2}\right)\overline{\boldsymbol{e}} \tag{12}$$

Here $\delta\tau(t) = 2\delta z(t)/c$ is the additional delay of the field induced by the mirror displacement and we neglected $O(\delta^2)$ effects. Note that the average part is unchanged, while the fluctuating one gets a contribution proportional to the average field and perpendicular to it: as expected, the mirror movement generates phase fluctuations.

The mirror moves for several reasons: it can be affected by noises such as seismic or thermal, and hopefully it can respond to the tidal effect of a gravitational wave. The field itself act on

IOP Conf. Series: Journal of Physics: Conf. Series **880** (2017) 012007 doi:10.1088/1742-6596/880/1/012007

the mirror with a radiation pressure force, which is proportional to the square of the field, whose fluctuating part will be given, after an average over ω_0^{-1} timescales, by

$$\delta F_{RP} = \chi \left[\overline{\boldsymbol{e}}^T \delta \boldsymbol{e}\,(t) + \overline{\boldsymbol{e}}'^T \delta \boldsymbol{e}'\,(t) \right] \tag{13}$$

Note that δF_{RP} is proportional to the field's fluctuations parallel to $\overline{\boldsymbol{e}}$, namely to amplitude fluctuations. The mirror will respond to external forces with something like

$$\delta z(t) = \mathcal{G} \star (\delta F_{RP} + \delta F)\,(t) = \mathcal{G} \star \left[2\chi \overline{\boldsymbol{e}}^T \delta \boldsymbol{e} + \delta F \right] (t) \tag{14}$$

where $\mathcal{G}$ is the appropriate mechanical Green function. Together with Equation (12) this gives

$$\delta \boldsymbol{e}'(t) \simeq \delta \boldsymbol{e}(t) + \overline{\boldsymbol{e}} \frac{2\omega_0}{c} \mathbb{R}\left(\frac{\pi}{2}\right) \mathcal{G} \star \left(2\chi \overline{\boldsymbol{e}}^T \delta \boldsymbol{e} + \delta F \right) \tag{15}$$

The fields near the two mirrors inside an optical cavity are related by

$$\delta \boldsymbol{e}_{IM} = \mathbb{T}\,(\mathbb{I} + \mathbb{M}_B \star)\,\delta \boldsymbol{e}_{EM} + \mathbb{T}\boldsymbol{g}_{EM} \star \delta F \tag{16}$$

$$\delta \boldsymbol{e}_{EM} = t\mathbb{T}\delta \boldsymbol{e}_{IM} + r\mathbb{T}\,(\mathbb{I} - \mathbb{M}_A \star)\,\delta \boldsymbol{e}_{IM} \tag{17}$$

Here we introduced a matrix which describes the modulation introduced by the mirror J

$$\mathbb{M}_J \equiv \frac{4\chi\omega_0}{c} \mathbb{R}\left(\frac{\pi}{2}\right) \mathcal{G}_J \overline{\boldsymbol{e}}_J \overline{\boldsymbol{e}}_J^T \tag{18}$$

a vector which describes the coupling to an external force applied to the mirror

$$\boldsymbol{g}_J \equiv \frac{2\omega_0}{c} \mathbb{R}\left(\frac{\pi}{2}\right) \overline{\boldsymbol{e}}_J \mathcal{G}_J \tag{19}$$

and a time delay operator $\mathbb{T}$ defined by its action

$$\mathbb{T}\delta \boldsymbol{e}(t) \equiv \mathbb{R}_c \delta \boldsymbol{e}\left(t - \frac{L}{c} \right) \tag{20}$$

which represents a propagation from one mirror to the other ($\mathbb{R}_c = \mathbb{R}(\omega_0 L c^{-1})$).

The front mirror IM, which is used to inject an external field $\delta \boldsymbol{e}_{IN}$, is described by the reflection and transmission coefficients r, t. The end mirror EM is supposed to be completely reflective and an external force δF is applied to it. By solving for the fields we get

$$\delta \boldsymbol{e}_{IM} = t\mathbb{C}^{-1}\mathbb{T}\,(\mathbb{I} + \mathbb{M}_B \star)\,\mathbb{T}\delta \boldsymbol{e}_{IN} - \mathbb{C}^{-1}\mathbb{T}\boldsymbol{g}_{EM} \star \delta F \tag{21}$$

$$\delta \boldsymbol{e}_{EM} = t\mathbb{C}^{-1}\mathbb{T}\delta \boldsymbol{e}_{IN} + r\mathbb{C}^{-1}\mathbb{T}\,(\mathbb{I} - \mathbb{M}_A \star)\,\mathbb{T}\boldsymbol{g}_{EM} \star \delta F \tag{22}$$

where

$$\mathbb{C} = \mathbb{I} - r\mathbb{T}\,(\mathbb{I} + \mathbb{M}_B \star)\,\mathbb{T}\,(\mathbb{I} - \mathbb{M}_A \star) \tag{23}$$

and finally we can write the field exiting from the cavity as a function of the incoming one

$$\delta \boldsymbol{e}_{OUT} = \mathbb{C}^{-1} \left\{ \left[\mathbb{T}\,(\mathbb{I} + \mathbb{M}_{EM} \star)\,\mathbb{T} - r\,(\mathbb{I} + \mathbb{M}_{IM} \star) \right] \delta \boldsymbol{e}_{IN} - t\mathbb{T}\boldsymbol{g}_{EM} \star \delta F \right\} \tag{24}$$

In order to interpret in the correct way these expressions we need also the values of the mean fields near the mirrors. These are given by a set of equations completely equivalent to (21) and (22), but with $\mathbb{T} = \mathbb{R}_c$, $\mathbb{M}_J = 0$ and $\delta F = 0$. The final result is

$$\overline{\boldsymbol{e}}_{IM} = t\left(1 - r\mathbb{R}_c^2\right)^{-1} \mathbb{R}_c^2 \overline{\boldsymbol{e}}_{\mathrm{IN}} \tag{25}$$

$$\overline{\boldsymbol{e}}_{EM} = t\left(1 - r\mathbb{R}_c^2\right)^{-1} \mathbb{R}_c \overline{\boldsymbol{e}}_{\mathrm{IN}} \tag{26}$$

IOP Conf. Series: Journal of Physics: Conf. Series **880** (2017) 012007 doi:10.1088/1742-6596/880/1/012007

This relatively compact expression contains a rich phenomenology. By choosing appropriately the reference frame we can couple the cavity to a gravitational wave writing

$$\delta F = \frac{1}{2} L\ddot{h} \tag{27}$$

where h is the strain induced in the direction of the cavity. In this way we can compare the noise and the signal of the cavity, by looking at the first and second term on right side of Equation (24). I will restrict to the particular case of a cavity with $\mathcal{G}_{IM} = \mathcal{G}_{EM} \equiv \mathcal{G}$ at the resonance (which means $\mathbb{R}_c = \mathbb{I}$). For simplicity I will consider also only the high finesse ($t \ll 1$) and quasistatic ($\Omega L/c \ll 1$) regime. In the frequency domain we get

$$\delta\tilde{\boldsymbol{e}}_{OUT} \simeq \delta\boldsymbol{e}_{IN} + \frac{4\omega_0}{c}\frac{\mathbb{R}\left(\frac{\pi}{2}\right)\overline{\boldsymbol{e}}_{\rm IN}}{1-r}\tilde{\mathcal{G}}\left(\Omega\right)\left(2\chi\overline{\boldsymbol{e}}_{\rm IN}^{T}\delta\tilde{\boldsymbol{e}}_{\rm IN} + \frac{L}{2}\Omega^2\delta\tilde{h}\right) \tag{28}$$

A quantum description of the system can be obtained by promoting the fluctuating fields $\delta\boldsymbol{e}(t)$ to operators $\delta\hat{\mathbf{e}}(t)$ with appropriate commutation relations. As a consequence of these the two components of $\delta\hat{\mathbf{e}}(t)$ can't be measured with arbitrary precision at the same time: quantum fluctuations will always be present, will be characterized by the symmetrized expectation values

$$\mathbb{K}\left(t-t'\right) = \left\langle \delta\hat{\mathbf{e}}(t)\delta\hat{\mathbf{e}}(t')\right\rangle_{symm} \tag{29}$$

whose Fourier transform can be interpreted as a noise power spectrum.

The laser beam used in gravitational detectors can be modeled as a a single mode of the electromagnetic field in a coherent state. Coherent states are minimum uncertainty states, because they saturate the Heisenberg uncertainty relations. In particular they are a "fair" compromise between phase and amplitude indeterminacy of the field, and in this sense they can be seen as the "most classical" states of light. Whatever quadrature we choose to measure, we will obtain the same noise.

If we look at Equation (28) we see that the measurement which maximize the signal must be done in the direction perpendicular to $\overline{\boldsymbol{e}}_{\rm IN} = \overline{\boldsymbol{e}}_{\rm OUT}$, which is the direction associated to phase fluctuations. The terms proportional to $\delta\boldsymbol{e}_{\rm IN}$ are noise contributions. the first from the left comes from the input phase fluctuations, which are simply reflected by the cavity, and can be interpreted as shot noise. The second is generated by the back action of the radiation pressure on the mirror, and is called radiation pressure noise. The third term is the signal. Note that, as I said, the ratio between the signal and the shot noise can be reduced by increasing the amplitude of the input field. However when we do this we reduce the ratio between the signal and the radiation pressure noise, as this one is proportional to the second power of the input field. It seems that there is a fundamental limit (which is called *standard quantum limit)* set by quantum noise which cannot be evaded. As a matter of fact this is not true.

4.2. Squeezed states

If we look again at Equation (28) and we analyze the results of a measurement of a generic quadrature, we find a surprising result. It comes out that the quadrature which maximize the ratio between signal and quantum noise is not the phase one. The reason is that the output field $\delta\boldsymbol{e}_{\rm OUT}$ is not in a coherent state, but in a squeezed one.

There is a particular class of squeezed states whose members share with the coherent states the minimum uncertainty property. They can have, for example, a reduced phase uncertainty at the expense of a larger amplitude one (see Figure 3). In that case for a given value of the laser power the shot noise (connected with phase indeterminacy) will be reduced.

A qualitative representation of coherent and squeezed state in the quadrature space, which can be seen as the analogous of the classical phase space for an harmonic oscillator, is given

IOP Conf. Series: Journal of Physics: Conf. Series **880** (2017) 012007 doi:10.1088/1742-6596/880/1/012007

in Figure (3). It comes out that fluctuation of coherent and squeezed states are Gaussian. For this reason the fluctuation of a coherent state is represented by a circle which indicates the uncertainty region of the field (the indeterminacy of both quadratures δp and δq are the same and are uncorrelated). A squeezed state is represented by an ellipse, with a fluctuation reduced along one quadrature and increased along the other. The phase fluctuation $\delta\phi_-$ can be reduced both by increasing the laser power ($\delta\phi_+ < \delta\phi_-$) or by appropriately squeezing the state ($\delta\phi_{ps} < \delta\phi_-$). The appropriate tool to give a well defined meaning to the error ellipse is the Wigner quasi-probability functions, which for coherent and minimum uncertainty squeezed states is Gaussian.

In the case of $\delta\boldsymbol{e}_{\mathrm{OUT}}$ the squeezing is generated by the back action of the radiation pressure, and is frequency dependent. In other words, if we evaluate the Fourier transform of the correlation matrix (29) we obtain a frequency dependent spectral covariance matrix. Typically when the mechanical response of the apparatus described by $\mathcal{G}$ is large (for example near a resonance or in the low frequency region for a free mass) back action (ponderomotive) effects become large and we obtain a strongly stretched ellipse.

The idea of using squeezed light to improve the sensitivity of an interferometric detector of gravitational waves is around since a long time [10], and the possibility of measuring an optimized quadrature is just one of the possible options.

Squeezed states of light can be produced routinely today, with increasing squeezing levels. The main difficulty is to produce squeezing in the frequency range of interest, which is the audio region for earth bound detectors. But progresses are quite fast.

By injecting a squeezed vacuum in an interferometer it is possible to evade the standard quantum limit [11, 12, 13], and the reduction of shot noise will be pursued by both LIGO and VIRGO using this technique. It is also possible in principle to completely eliminate radiation pressure effects by a combination of squeezed vacuum injection and output quadrature optimization [13].

4.3. Optomechanical effects

Several other techniques for evading the standard quantum limit have been demonstrated theoretically in several papers. It can be shown that in the low photon number regime the optimal states are the Fock ones [14, 15]. When the number of photons involved is high, the optimal approach is based on squeezed states [16].

A general observation is that the final sensitivity depends on both the optical degrees of freedom of the apparatus and the mechanical ones. These are coupled by radiation pressure, which acts in a dual way:

- The quantum state of the optical modes can be changed by the back action of the mechanical degrees of freedom. For example a mirror recoiling under the action of the radiation pressure fluctuation can induce a phase fluctuation on the reflected beam correlated with the first, generating a squeezed state (*ponderomotive squeezing*). In the general case, within the linearized approximation for a simple cavity, this effect is completely described by Equation (24), once the appropriate parameters of the cavity are inserted.
- The dynamic of the mirrors can be changed. For example the radiation present inside a slightly out of resonance (detuned) cavity can produce a considerable effective mechanical stiffness, the so-called *optical spring effect.* This effect is also implicitly contained inside Equation (24), but can be understood simply by looking at the poles of the transfer function, which are the solution of $\det\mathbb{C} = 0$ (see Equation (23)). These can be associated to the modes of the cavity, and in the general case will be determined by both mechanical and optical effects. In particular a force on the mirror IM can have an effect, mediated by the radiation pressure, on the mirror EM. Delay effects can also induce damping (or anti-damping) effects, and instabilities can appear.

IOP Conf. Series: Journal of Physics: Conf. Series **880** (2017) 012007 doi:10.1088/1742-6596/880/1/012007

The study of optomechanical effects is an active field of research, which is connected with fundamental questions about the foundations of quantum mechanics and quantum information. It is also expected to produce an increasing quantity of technological applications. Usually the most accessible examples of optomechanical devices are small scale ones (such as for example microcavities). A relevant point to be stressed is that in the case of gravitational waves detectors we deal with macroscopic masses, and in principle we have the possibility of studying quantum mechanical effects, such as entanglement [17], in this regime.

The direct observation of the ponderomotive squeezing effect is of great interest. Several attempts have been made, and a number of experiments are currently in various phases of their development. The effect has been observed on membranes [18] and using an optomechanical cavity coupled to a waveguide [19]. Direct evidence of ponderomotive squeezing is still lacking in macroscopic optical cavities.

There are other possible schemes for standard quantum limit evasion. Of particular interest are optical schemes based on the Sagnac effect [20] which are intrinsically unaffected by back action effects, and can be seen as examples of *Quantum Non Demolition* measurements. Other examples are schemes which exploit the *optical spring effect* previously mentioned [21, 22, 23]. Both approaches are starting to become technically feasible.

4.4. Squeezing and thermal noise

The interaction of the system with the environment can be modeled, via the fluctuation dissipation theorem, by introducing appropriate external stochastic forces. It is intuitive (and can be explicitly verified by looking at Equation (15)) that these external forces will introduce an additional phase noise. The interplay between optical noise and thermal noise is not completely trivial when squeezed light is used, and the optimal strategies to be used in order to improve the sensitivity must be carefully designed.

A point worth to be mentioned is that in presence of an optical spring the evaluation of thermal noise must be done with care. In particular, the mechanical response of the system that must be used to apply the fluctuation dissipation theorem must not take into account the optical stiffness. The reason for that can be understood intuitively because the source of optical stiffness is the laser electromagnetic field inside the cavity, which can't be seen as a system in thermal equilibrium with the environment.

This can be exploited to reduce thermal noise in the frequency domain of interest. For example it is possible to push the resonance of a system to higher frequencies adding an optical spring constant to the mechanical one. Modeling the mechanical damping with a loss angle ϕ we can write

$$K_{eff} = K_{mech} (1 + i\phi) + K_{opt} \tag{30}$$

and when $K_{opt} \gg K_{mech}$ we obtain a large Q factor by a kind of "dilution effect". As a side note, the application of the fluctuation dissipation effect in a situation which cannot be strictly defined of thermodynamic equilibrium is by itself an interesting subject in my opinion worth of further theoretical and experimental investigation.

4.5. Squeezing and losses

In order to use squeezed states of light a particular care should be used in order to avoid optical losses due to absorption or scattering. These deteriorate the squeezing level and the problem is particularly relevant because the implementation of standard quantum limit evasion requires often additional optical elements.

When there are optical losses inside the apparatus a quantum description becomes somewhat subtle. The main issue is that quantum mechanics must be unitary, and this is not compatible with a naive description. It is easy to understand the point using a simple model. Suppose that a field described by an operator $\hat{a}$ is transmitted and partially absorbed through a lens. One could be tempted to describe the transmitted field with an operator

$$\hat{b} = \sqrt{1-\eta^2}\hat{a} \tag{31}$$

where η parametrize the loss. However the commutation rules of this operator can't be canonical:

$$\left[\hat{b}, \hat{b}^\dagger\right] = \left(1-\eta^2\right)\left[\hat{a}, \hat{a}^\dagger\right] \neq \left[\hat{a}, \hat{a}^\dagger\right] \tag{32}$$

In the correct modelization we must look at the absorbed field of the mode $\hat{a}$ as to a scattered one in another mode $\hat{a}_s$. And the same mechanism which produces this scattering will be able to scatter a mode $\hat{b}_s$ into the mode $\hat{b}$. The correct description will be

$$\hat{b} = \sqrt{1-\eta^2}\hat{a} - \eta\hat{b}_s \tag{33}$$

$$\hat{a}_s = \eta\hat{a} + \sqrt{1-\eta^2}\hat{b}_s \tag{34}$$

and it is easy to verify that the commutation rules are preserved.

A practical consequence of this is that if $\hat{a}$ describes a carefully prepared squeezed state, after the loss the squeezing of the field $\hat{b}$ will be reduced. The reason is that $\hat{b}_s$ will describe a non squeezed vacuum state, and his fluctuations will add to the ones of $\hat{a}$.

5. The first detection

The first direct detection of a gravitational wave signal was made by the two LIGO interferometers on September 14, 2015 [24]. The signal where detected first by the LIGO Livingston Observatory, and then with a relative delay of 7ms by the LIGO Hanford Observatory. The signal to noise ratio was quite high, of about 24, and allowed for a determination of the main parameters of the event with a good confidence.

The source was identified as a binary coalescence of two black holes[25, 24], with masses of $36.2^{+5.2}_{-3.8}\,M_\odot$ and $29.1^{+3.7}_{-4.4}M_\odot$. The remnant of the coalescence is a Kerr black hole of $62.3^{+3.7}_{-3.1}M_\odot$. The spins of the final black hole was determined to be about $0.68^{+0.005}_{-0.06}$, while the determination of the spin of the two initial objects was much less accurate.

Looking at the initial and final masses, it comes out that the energy radiated by the system, almost completely in the last 0.5s of the coalescence, was of about $3^{+0.5}_{-0.4}M_\odot c^2$. For a system of two black holes the only expected mechanism for energy loss is toward emission of gravitational waves.

Using the observed delay between the H1 and L1 signals and the constraint about the consistence between the two waveforms it was possible to constrain the position in the sky of the source in a fraction of an annulus of about 230deg^2, which is quite large but it is the best that can be done with a pair of detectors. Finally, the event happened at a redshift of $z = 0.09^{+0.03}_{-0.04}$, which correspond to a distance of about 1.3×10^9 ly from us.

The total time spent inside the sensitivity band of the detectors was about 0.5s. The reason is that the mass of the coalescing objects was quite large, with an higher frequency cut-off quite low[2].

There is a good agreement between the observed signal and the prediction of general relativity. Owing to its good signal to noise ratio it was possible to make several tests, in particular by looking at the merger regime where nonlinear effects are expected to be relevant and in the final phase (the so-called ring down) which is dominated by the relaxation of a small number of excitation of the final Kerr black hole. These are under good theoretical control, and give a signature of the validity of the theory. During the first observing run a second black hole coalescence ($14.2M_\odot + 7.5M_\odot \to 21.8M_\odot$) was clearly observed.

[2] This can estimated by using Eq. (6), or just looking at Figure 4. Remember that Eq. (6) is strictly valid only in the test mass approximation.

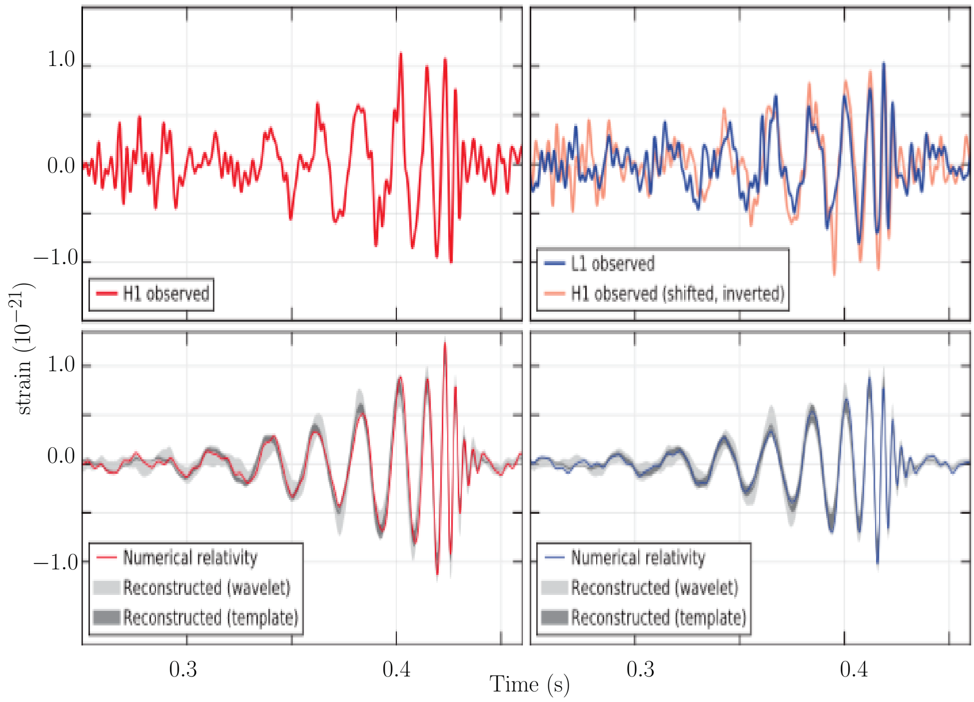

Figure 4. Plots of the signal of the first gravitational wave direct detection. On the top left, the signal measured at the LIGO Hanford Observatory (H1). Noise at frequencies different from the signal's ones have been filtered out. On the top right, the signal measured at the LIGO Livingston Observatory (L1) overimposed with the H1 one, after the compensation of the observed delay and of an expected sign flip. On the bottom, the measured signals compared with the prediction of numerical relativity. Adapted from [24].

6. Conclusions and perspectives

For the first time a gravitational wave signal has been directly detected. At present, a couple of binary black hole coalescences were seen, but this is just one example of a large set of possible sources. We are confident that in a short time a coalescence between a pair of neutron stars (or between a neutron star and a black hole) will be detected. This will open the possibility of studying the equation of state of the matter in the extreme conditions that can be found in the interior of a neutron star, which will give important information about fundamental physics. Other sources are expected, as I discussed, and maybe something completely unexpected can happen. In short, it can be said that we are at the beginning of the gravitational wave astronomy era.

If we look at the predictions about the future improvement of sensitivity of earth bound detectors, we can say that in the next few years with advanced detectors we will be able probably to detect $O(10^2)$ events similar to the one of the first detection. This can appear surprising, but we should remember that the volume of the universe explored is proportional to the third power of the sensitivity.

This year Advanced VIRGO will join the network of observatories, and is expected to give an important contribution, especially for the determination of the parameters of the sources. In 2018 KAGRA, a cryogenic Japanese detector, is expected to join also, and probably a fifth one (LIGO India) will start its operations after 2020.

Still larger improvements are foreseen for the so called *third generation detectors*, such as the *Einstein Telescope* [26]. In this case it is possible that optical noise will become the most fundamental limit of sensitivity for the detector both at higher and lower frequencies [27]. Another important sensitivity limitation will become the so-called Newtonian noise. This could be described as the effect of direct gravitational coupling between the apparatus and environmental density fluctuations. It is possible that its effect could be seen in advanced detectors also (see Figure 2) and the study of possible methods for its mitigation is already started (see [28] for a review).

Newtonian noise can be seen as a fundamental limit that make difficult to push the detection window to lower frequencies for an earth bound experiment. The LISA project [29] for a space based observatory will be immune to seismic and Newtonian noise. Its long baseline will allow for a sensitivity window between 10^{-3}Hz and 1Hz. It will be complementary to earth bound detector, and it will allow to study very massive black holes coalescences and cosmological stochastic background in particular.

Acknowledgments
I wish to thank the organizers of DICE workshop for inviting me, and for their patience waiting the preparation of this paper.

References

[1] Einstein A 1916 Näherungsweise Integration der Feldgleichungen der Gravitation *Sitzungsberichte der Königlich Preussischen Akademie der Wissenschaften Berlin* **688**
[2] Einstein and Rosen N 1937 On Gravitational Waves *Journal of the Franklin Institute* **223** 43
[3] Einstein A, Infeld L and Hoffmann B 1938 The Gravitational Equations and the Problem of Motion *Annales of Mathematics* **39** 65
[4] Weisberg J M and Taylor J H 2005 The Relativistic Binary Pulsar B1913+16: Thirty Years of Observations and Analysis *In Binary Radio Pulsar, ASP Conference Series. Eds. F. A. Rasio and I. H. Stairs* **328** 25
[5] Aasi J et al. (The LIGO Scientific Collaboration) 2015 Advanced LIGO *Class. Quantum Grav.* **32** 074001
[6] Acernese F et al. (VIRGO Collaboration) 2015 Advanced Virgo: a second-generation interferometric gravitational wave detector *Class. Quantum Grav.* **32** 024001
[7] Jones D I 2002 Gravitational waves from rotating strained neutron stars *Class. Quantum Grav.* **19** 1255
[8] Maggiore M 2000 Gravitational wave experiments and early universe cosmology *Physics Reports* **331** 283
[9] Braginsky V B, Strigin S E and Vyatchanin S P 2001 Parametric oscillatory instability in Fabry–Perot interferometer *Phys. Lett. A* **287** 331
[10] Caves C M 1981 Quantum mechanical noise in an interferometer *Phys. Rev. D* **23** 1693
[11] Yuen H P 1983 Contractive States and the Standard Quantum Limit for Monitoring Free-Mass Positions *Phys. Rev. Lett.* **51** 719
[12] Jaekel M T and Reynaud S 1990 Quantum Limits in Interferometric Measurements *Europhys. Lett.* **13** 301
[13] Kimble H J, Levin Y, Matsko A B, Thorne K S, and Vyatchanin S P 2001 Conversion of conventional gravitational-wave interferometers into quantum nondemolition interferometers by modifying their input and/or output optics *Phys. Rev. D* **65** 022002
[14] Mitchell M W, Lundeen J S and Steinberg A M 2004 Super-resolving phase measurements with a multiphoton entangled state *Nature* **429** 161
[15] Rarity J G, Tapster P R, Jakeman E, Larchuk T, Campos R A, Teich M C, and Saleh B E A 1990 Two-photon interference in a Mach-Zehnder interferometer *Phys. Rev. Lett.* **65** 1348
[16] Demkowicz-Dobrzański R, Banaszek K and Schnabel R 2013 Fundamental quantum interferometry bound for the squeezed-light-enhanced gravitational wave detector GEO 600 *Phys. Rev. A* **88** 041802
[17] Müller-Ebhardt H, Rehbein H, Schnabel R, Danzmann K and Chen Y 2008 Entanglement of macroscopic test masses and the Standard Quantum Limit in laser interferometry *Phys. Rev. Lett.* **100** 013601
[18] Purdy T P et al. 2013 Observation of Radiation Pressure Shot Noise on a Macroscopic Object *Science* **339** 801
[19] Safavi-Naeini A H, Gröblacher S, Hill J T, Chan J, Aspelmeyer M and Painter O 2013 Squeezed light from a silicon micromechanical resonator *Nature* **500** 185
[20] Eberle T et al. 2010 Quantum Enhancement of the Zero-Area Sagnac Interferometer Topology for Gravitational Wave Detection *Phys. Rev. Lett.* **104** 251102
[21] Buonanno A and Chen Y 2002 Signal recycled laser-interferometer gravitational-wave detectors as optical springs *Phys. Rev. D* **65** 042001

[22] Sheard B S, Gray M B, Mow-Lowry C M, McClelland D E, and Whitcomb S E 2004 Observation and characterization of an optical spring *Phys. Rev. A* **69** 051801

[23] Corbitt T, Wipf C, Bodiya T, Ottaway D, Sigg D, Smith N, Whitcomb N and Mavalvala N 2007 Optical Dilution and Feedback Cooling of a Gram-Scale Oscillator to 6.9mK *Phys. Rev. Lett.* **99** 160801

[24] Abbott B P et al. (LIGO Scientific Collaboration and Virgo Collaboration) 2016 Observation of Gravitational Waves from a Binary Black Hole Merger *Phys. Rev. Lett.* **116** 061102

[25] Abbott B P et al. (LIGO Scientific Collaboration and Virgo Collaboration) 2016 Binary Black Hole Mergers in the First Advanced LIGO Observing Run *Phys. Rev. X* **6** 041015

[26] Punturo M et al. 2010 The third generation of gravitational wave observatories and their science reach *Class. Quant. Grav.* **27** 084007

[27] Hild S et al. 2010 A xylophone configuration for a third-generation gravitational wave detector *Class. Quantum Grav.* **27** 015003

[28] Harms J 2015 Terrestrial Gravity Fluctuation *Living Rev Relativ* **18** 3

[29] Jennrich O 2004 LISA: a mission to detect and observe gravitational waves *In Gravitational Wave and Particle Astrophysics Detectors, edited by James Hough, Gary H. Sanders, Proceedings of SPIE* **5500**